

Femtosecond Laser Inscription of Fiber Bragg Grating in Twin-Core Few-Mode Fiber for Directional Bend Sensing

Kaiming Yang, Jun He, *Member, OSA*, Changrui Liao, Ying Wang, Shen Liu, Kuikui Guo, Jiangtao Zhou, Zhengyong Li, Zhan Tan, and Yiping Wang, *Senior Member, OSA/IEEE*

Abstract—We demonstrated femtosecond laser inscription of fiber Bragg gratings (FBGs) in a twin-core few-mode fiber (TC-FMF) for directional bend sensing. An FBG was selectively inscribed in one core of the TC-FMF by using an 800 nm femtosecond laser through a phase mask. Three resonance peaks at the wavelengths of 1549.05, 1547.65, and 1546.08 nm were observed in the reflection spectrum of the TC-FM FBG, and were generated by the LP_{01} mode resonance, LP_{01} – LP_{11} mode cross-coupling resonance, and LP_{11} mode resonance, respectively. Moreover, the TC-FM FBG exhibited the capability of directional bend sensing and achieved a maximum bend sensitivity of -37.41 pm/m^{-1} . Hence, the proposed TC-FM FBG directional bend sensors could further be developed as promising solutions for detecting vectorial seismic or acoustic waves and 3-D shape sensing.

Index Terms—Fiber Bragg gratings, fiber optics sensors, ultrafast lasers.

I. INTRODUCTION

IN RECENT years, tremendous progress has been made in both spatial-division-multiplexing (SDM) transmission and mode-division-multiplexing (MDM) transmission due to the limit in the bandwidth of a single-mode fiber (SMF) [1]–[3]. Multi-core fiber (MCF), few-mode fiber (FMF), and the related fiber devices are the foundation of the SDM and MDM transmission systems. Fiber Bragg gratings (FBGs) inscribed in various MCFs and FMFs has been reported during the past decade. For instance, Flockhart *et al.* inscribed three FBGs in a four-core

fiber by use of a UV laser through a phase mask [4]. Lindley *et al.* demonstrated uniform multicore FBGs via optimized UV illumination and achieved high-reflectivity, narrow-bandwidth FBGs in the outer six cores of a seven-core fiber at a constant wavelength [5]. Stepień *et al.* reported FBGs in all of the seven cores of a hole-assisted multicore fiber after one inscription process with a KrF excimer laser in a Talbot interferometer set up [6]. Researchers from OFS Labs demonstrated the fabrication of seven phase-shifted FBGs in a hexagonally arrayed Er-doped multicore fiber and hence achieved parallel-integrated distributed feedback (DFB) fiber lasers [7]. Moreover, the inscription of few-mode FBGs has also been studied in the past few years. Few-mode FBGs were fabricated by focusing UV laser beam onto different types of FMFs [8]–[11], and could be developed for fiber-optic sensors [8], [9] and novel fiber lasers [12]. In general, FBGs were successfully fabricated in both MCFs and FMFs. Recently, multicore few-mode fibers (MC-FMFs) were created to further increase the transmission capacity by combining the SDM and MDM together [2], [3]. Nevertheless, as far as we are concerned, FBGs inscribed in MC-FMFs have never been reported yet.

Apart from the applications in optical fiber communication systems, the FBGs inscribed in MCFs and FMFs could also be developed for fiber-optic sensors, especially for directional bend sensors [4], [13]–[18]. It is well known that curvature measurement plays important roles in many engineering fields, such as aerospace, robotics, biomedical instruments, and structural health monitoring. Various fiber-optic sensing devices were studied to create directional bend sensors, including long-period fiber gratings [19], [20], tilted FBGs [21], cladding waveguide FBGs [22], multicore fiber gratings [4], [13]–[18], and in-fiber modal interferometers based on photonic crystal fibers [23], [24] or multimode fibers [25]. Among these fiber bend sensors, FBG-based bend sensors have the advantages of wavelength encoding and capability of multiplexing. In 2000, Gander *et al.* first reported a bend sensor based on a multicore FBG [13]. Subsequently, Flockhart *et al.* achieved a two-axis vector bend sensor by employing three FBGs inscribed in a four-core fiber [4]. And then, Silva-López *et al.* measured orientated transverse load by using two FBGs in a four-core fiber [14], [15]. In addition, two-axis dynamic curvature measurements were also demonstrated [16], [17]. Recently, Zhang *et al.* reported a

Manuscript received June 14, 2017; revised August 21, 2017; accepted September 3, 2017. Date of publication September 7, 2017; date of current version October 12, 2017. This work was supported in part by the National Natural Science Foundation of China under Grants. 61505120, 61575128, 61425007, and 61635007, in part by Guangdong Natural Science Foundation under Grants 2015A030310243, 2017A010102015, 2014B050504010, 2015B010105007, and 2014A0303 08007, and in part by Science and Technology Innovation Commission of Shenzhen under Grants JCYJ20150324141711611, JCYJ20170302143105991, JCYJ20150324141711614, and JCYJ2015032414-1711576. (Kaiming Yang and Jun He contributed equally to this work.) (Corresponding authors: Yiping Wang and Jun He.)

The authors are with the Key Laboratory of Optoelectronic Devices and Systems of Ministry of Education and Guangdong Province, College of Optoelectronic Engineering, Shenzhen University, Shenzhen 518060, China (e-mail: yangkaiming@email.szu.edu.cn; hejun07@szu.edu.cn; cliao@szu.edu.cn; yingwang@szu.edu.cn; liushen.szu@gmail.com; 2150190116@email.szu.edu.cn; zhoujiangtao@email.szu.edu.cn; lizhengy88@126.com; tanzhan@email.szu.edu.cn; ypwang@szu.edu.cn).

Color versions of one or more of the figures in this paper are available online at <http://ieeexplore.ieee.org>.

Digital Object Identifier 10.1109/JLT.2017.2750407

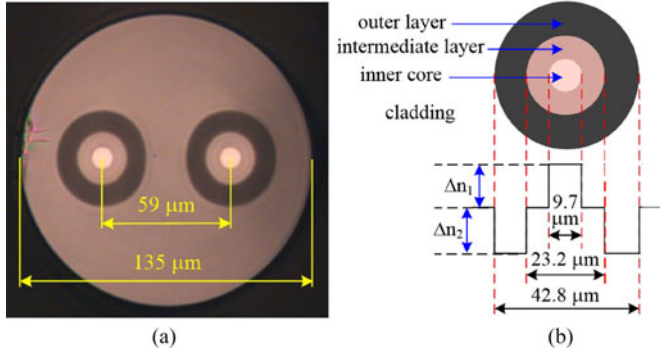


Fig. 1. Schematics of the twin-core few-mode fiber (TC-FMF). (a) Microscopic image of the cross-section of the TC-FMF. (b) Refractive index profiles of one fiber core of the TC-FMF.

directional bend sensor based on two FBGs inscribed in heterogeneous seven-core fiber using uniform UV illumination [18].

Most of the reported multicore gratings were inscribed by using UV laser illumination [4]–[7], [13]–[18]. However, the inscription of FBGs by employing UV laser always relies on the fiber photosensitivity, and hence could not be used for selectively inscribing FBGs in one specific core of multicore fiber. In addition to the UV laser, 800 nm NIR femtosecond laser was also demonstrated to inscribe FBGs in multicore mid-IR glass fibers by researchers from Aston University [26]. As a result of the laser beam scanning used in their work, three FBGs with similar Bragg wavelengths were inscribed simultaneously in each core of the three-core fibers, and hence could not be distinguished from each other.

In this paper, we demonstrated femtosecond laser inscription of FBGs in a TC-FMF for directional bend sensing. At first, we selectively inscribed an FBG in one core of the TC-FMF by using an 800 nm femtosecond laser through a phase mask. And then, we studied the mode excitation in the TC-FMF FBG via offset coupling. Three resonance peaks at the wavelengths of 1549.05, 1547.65, and 1546.08 nm were observed in the reflection spectrum, and were responsible for the LP_{01} mode resonance, LP_{01} - LP_{11} mode cross-coupling resonance, and LP_{11} mode resonance, respectively. Moreover, we studied the directional bend response of the TC-FM FBG, and demonstrated that the TC-FM FBG had a maximum bend sensitivity of -37.41 pm/m^{-1} and had the capability of directional bend sensing.

II. FBG INSCRIPTION IN TC-FMF

The TC-FMF used in our experiments was fabricated by YOFC in Wuhan, China. Fig. 1(a) shows the microscope image of the cross section of the TC-FMF. The TC-FMF has two fiber cores (i.e., core A and core B) and each fiber core consists of three layers: the inner core layer, the intermediate layer, and the outer layer. Fig. 1(b) illustrates the index profiles of the three layers of one fiber core. The inner core layer has a higher refractive index than fiber cladding and is responsible for guiding the light. The intermediate layer is composed of pure silica and has the same refractive index with fiber cladding. The outer layer has a lower refractive index, and is used as a depressed

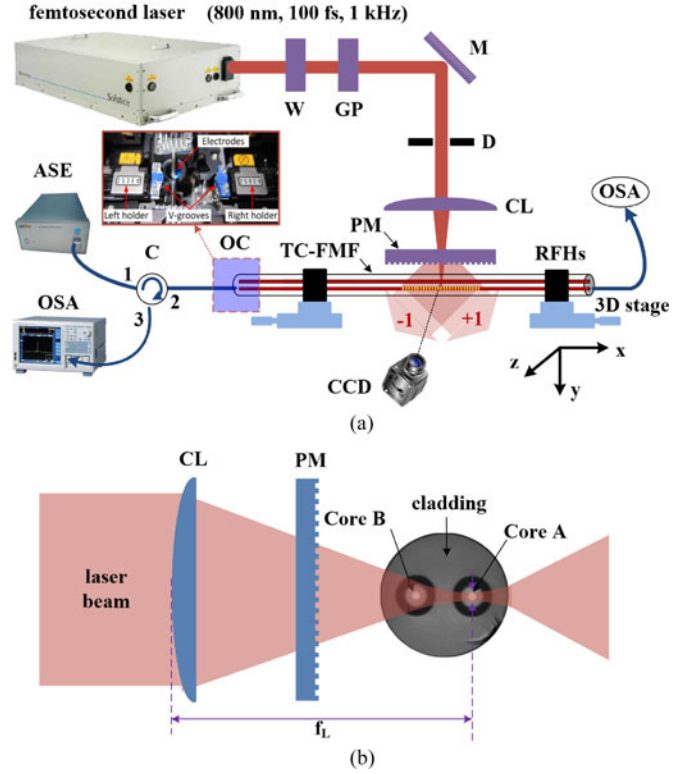


Fig. 2. Schematics of inscribing TC-FM FBGs by using femtosecond laser. (a) Experimental setup. (Inset: the offset coupling in a commercialized fusion splicer.) (b) Laser beam focusing geometry. (TC-FMF: twin-core few-mode fiber, W: waveplate, GP: Glan-polarizer, M: mirror, D: diaphragm, CL: cylindrical lens, PM: phase mask, RFHs: rotary fiber holders, ASE: amplified spontaneous emission, OSA: optical spectral analyzer, OC: offset coupling, C: circulator, CCD: charge coupled device, f_L : focal length.).

cladding trench. The overall fiber core diameter, inner core layer diameter, fiber cladding diameter, and the distance between core A and core B are about 42.8, 9.7, 135, and $59 \mu\text{m}$, respectively. Both fiber cores were designed for two modes operation, i.e., the fundamental core mode LP_{01} and the first-order higher core mode LP_{11} . Moreover, the large core-to-core distance and the depressed cladding trench ensure mode isolation between core A and core B in the TC-FMF.

Fig. 2(a) shows the experimental setup for inscribing TC-FM FBGs, which is similar to that presented in our previous works [27]–[29]. Femtosecond laser pulses with a wavelength of 800 nm, a pulse-width of 100 fs, a repetition rate of 1 kHz, and a pulse energy of 4 mJ were generated by a Ti:sapphire regenerative amplifier system (Spectra-Physics, Solstice). The laser was linearly polarized with a $1/e^2$ Gaussian diameter of 6.2 mm. The pulse energy was attenuated by rotating a half wave-plate followed by a Glan polarizer. As shown in Fig. 2(b), the laser beam was focused onto the TC-FMF using a cylindrical lens with a focal length of 50.2 mm through a uniform phase mask (Ibsen Photonics), which had a period of 1070 nm, a 0th order diffraction of below 4%, and an optimization for 800 nm TE illumination. The TC-FMF with coating removed was fixed behind the phase mask at a distance of $300 \mu\text{m}$ by using a pair of rotary fiber holders. The fiber holders were simultaneously rotated to ensure that the laser beam could propagate along the

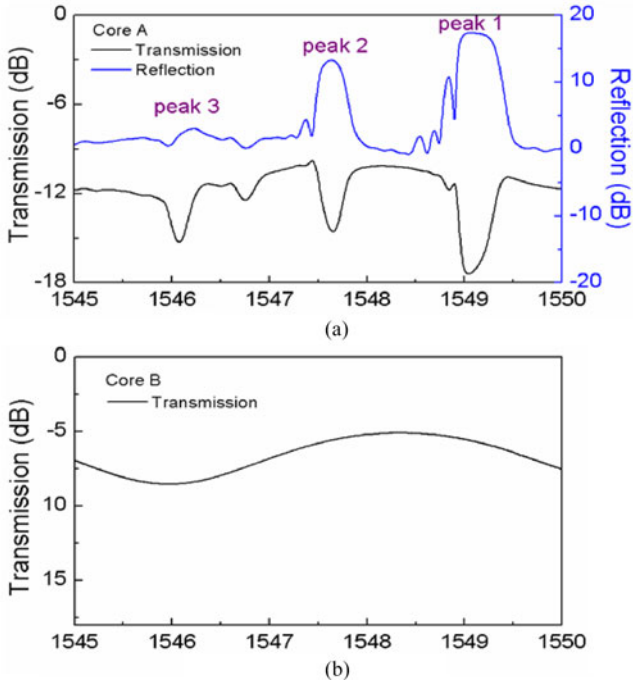


Fig. 3. Optical spectra of the TC-FM FBG. (a) Transmission and reflection spectra in core A of the TC-FMF. (b) Transmission spectrum in core B of the TC-FMF.

axis connecting core A and core B in the TC-FMF. Using Gaussian beam optics, the focal width and Rayleigh length of the laser beam were calculated to be 8.25 and 66.78 μm , respectively. Moreover, a SMF was offset-coupled to the core A of the TC-FMF by using a commercialized fusion splicer (Fujikura, ARC master, FSM-100P+). The transmission and reflection spectra of the TC-FM FBGs were measured by using an ASE light source together with an optical spectrum analyzer (Yokagawa AQ6370C) and a circulator.

The TC-FMF was H_2 -loaded at 100 bar, 80 $^\circ\text{C}$, for 7 days, and then an FBG was inscribed by means of focusing the femtosecond laser beam onto the core A of the H_2 -loaded TC-FMF. A pulse energy of 102 μJ and an exposure time of 30 s were used in TC-FM FBG inscription. Using Gaussian beam optics, the laser peak intensities at core A and core B were calculated to be 3.8×10^{12} and 2.0×10^{12} W/cm^2 , respectively [27], [30]. In case that the self-focusing effect [31] and the fiber lens effect [32] were taken into consideration, the laser intensity at core A will be even much higher than that at core B. As shown in Fig. 3, three resonance dips or peaks (i.e., peak 1, 2, and 3 at the wavelength of 1549.05, 1547.65, and 1546.08 nm, respectively) could be seen clearly in the transmission and reflection spectra in core A, whereas no resonance peak could be seen in the transmission spectrum in core B. It should be noted that 0 dB in the reflection spectra in this paper is the Fresnel reflection of fiber end of about 4%. Moreover, the fluctuations in the transmission spectra in Fig. 3 were resulted from the interference between two offset-coupled fiber ends and could disappear in the following steps via fusion splicing. The inscription of FBGs by using an 800 nm femtosecond laser was quite sensitive to the

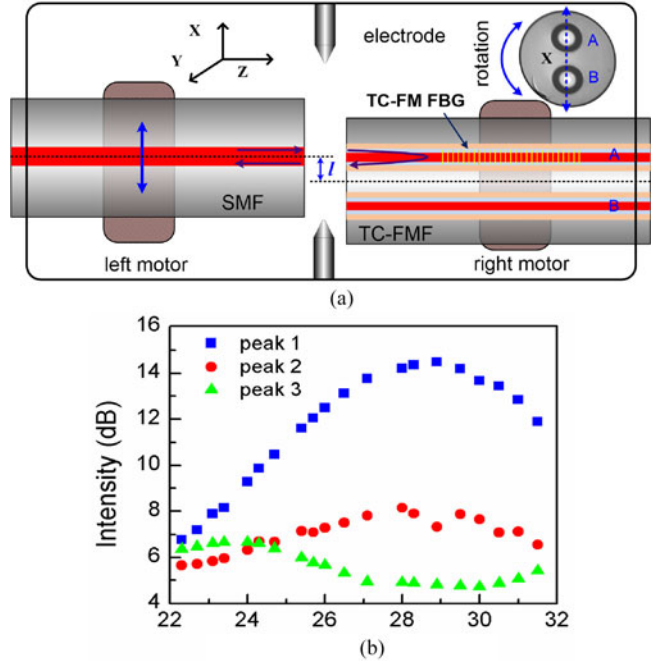


Fig. 4. Mode excitation in the TC-FM FBG via offset coupling. (a) Experimental setup for mode excitation in the TC-FM FBG by using a commercialized fusion splicer (Fujikura, ARC master, FSM-100P+). (b) The reflective intensities at three resonant wavelengths of the TC-FM FBG as a function of the lateral offset l between SMF and TC-FMF. (l : the lateral offset between the central axes of the SMF and the TC-FMF).

laser peak intensity due to its unique grating formation mechanism based on nonlinear multi-photon absorption together with a threshold effect [28], [30]. As a result, the 800 nm NIR femtosecond laser could be used to selectively inscribe an FBG in core A of the TC-FMF whereas with no FBG in core B.

III. MODE EXCITATION IN TC-FM FBG VIA OFFSET COUPLING

We further studied the mode excitation in the TC-FM FBG by use of a commercialized fusion splicer (Fujikura, ARC master, FSM-100P+). As shown in Fig. 4(a), at first, a SMF and the TC-FM FBG were placed in the left and right fiber holder of the fusion splicer, respectively. The SMF and TC-FMF were aligned to each other with the coincidence of their central axes. The distance between the ends of the SMF and the TC-FMF was set to be 2 μm . And then, as shown in the inset of Fig. 4(a), the TC-FM FBG was rotated by a rotary motor so that the axis connecting core A and core B could be aligned to the X direction in the fusion splicer. Subsequently, the SMF was precisely moved along the X direction by the left motor with a step of 0.1 μm , and hence the lateral offset l between the central axes of the SMF and the TC-FMF could be precisely adjusted. It could be seen from Fig. 4(b) that the reflective intensities at three resonant wavelengths, i.e., peak 1, 2, and 3, evolve differently with the variable lateral offset l . In case the offset l equals 24, 28, and 29 μm , the reflective intensity of peak 3, 2, and 1 reaches its maximum, respectively. Moreover, it should be noted that the SMF center aligns to the core A center in the case of l equals

29 μm and the SMF center aligns to the edge of the inner core layer of core A in the case of l equals 24 μm .

According to the theory used in previous works [8]–[11], the resonant wavelengths of peak 1 and 3 should be produced by the coupling between the forward and backward LP_{01} modes and the forward and backward LP_{11} modes, respectively. The resonant wavelength of peak 2 should be produced by the cross-coupling between the forward LP_{01} mode and backward LP_{11} mode and the cross-coupling between the forward LP_{01} mode and backward LP_{11} mode. The resonant wavelength λ_1 , λ_2 , and λ_3 of peak 1, 2, and 3 should be determined by phase match condition, and are given by

$$\lambda_1 = \lambda_{\text{LP}_{01}^+ \leftrightarrow \text{LP}_{01}^-} = 2n_{\text{eff},01}\Lambda, \quad (1)$$

$$\lambda_3 = \lambda_{\text{LP}_{11}^+ \leftrightarrow \text{LP}_{11}^-} = 2n_{\text{eff},11}\Lambda, \quad (2)$$

$$\begin{aligned} \lambda_2 &= \lambda_{\text{LP}_{01}^+ \leftrightarrow \text{LP}_{11}^-, \text{LP}_{11}^+ \leftrightarrow \text{LP}_{01}^-} \\ &= (n_{\text{eff},01} + n_{\text{eff},11})\Lambda = (\lambda_1 + \lambda_3)/2. \end{aligned} \quad (3)$$

where Λ is the grating pitch of the TC-FM FBG, and $n_{\text{eff},01}$, $n_{\text{eff},11}$ are the mode effective index for LP_{01} mode and LP_{11} mode, respectively. By taking experimental resonant wavelength into (1), (2), (3), $n_{\text{eff},01}$, $n_{\text{eff},11}$ are calculated to be 1.4477 and 1.4449, respectively.

From Fig. 4(b), we can see that the resonant coupling between LP_{01} modes can be excited most efficiently in the case of direct incidence, whereas the resonant coupling between LP_{11} modes will be excited most efficiently in the case of oblique incidence via offset coupling. As a result, we set the lateral offset l to be 25.4 μm to obtain both efficient LP_{01} mode resonance and efficient LP_{11} mode resonance, and then spliced the SMF and the TC-FMF together in the fusion splicer. Fig. 5(a) and (b) exhibit the reflection spectra of TC-FM FBG before and after splicing, respectively. It is obvious that the LP_{11} mode resonance and the LP_{01} – LP_{11} mode cross-coupling resonance were further enhanced by the fusion splicing process.

Furthermore, we investigated the thermal response of the three reflective resonance peaks by means of placing the TC-FM FBG into an electrical oven (LCO 102) and raising gradually the temperature from room temperature to 100 $^\circ\text{C}$ with a step of 10 $^\circ\text{C}$. As shown in Fig. 5(c), all the three resonant wavelengths show excellent linearity with slightly different temperature sensitivities of 9.86, 10.31, and 9.55 $\text{pm}/^\circ\text{C}$ for LP_{01} mode resonance, LP_{01} – LP_{11} mode cross-coupling resonance, and LP_{11} mode resonance, respectively.

IV. DIRECTIONAL BEND RESPONSE OF TC-FM FBG

We investigated the directional bend response of the TC-FM FBG via the experimental setup shown in Fig. 6(a). The TC-FM FBG was fixed by a pair of rotary fiber holders (Newport model 466A-718), which were separately mounted on a pair of 3D translation stages. The bend curvature of the TC-FM FBG could be changed either by altering the fiber length fixed between the two fiber holders or by moving the translation stages. The bend direction could be changed by rotating the two fiber holders

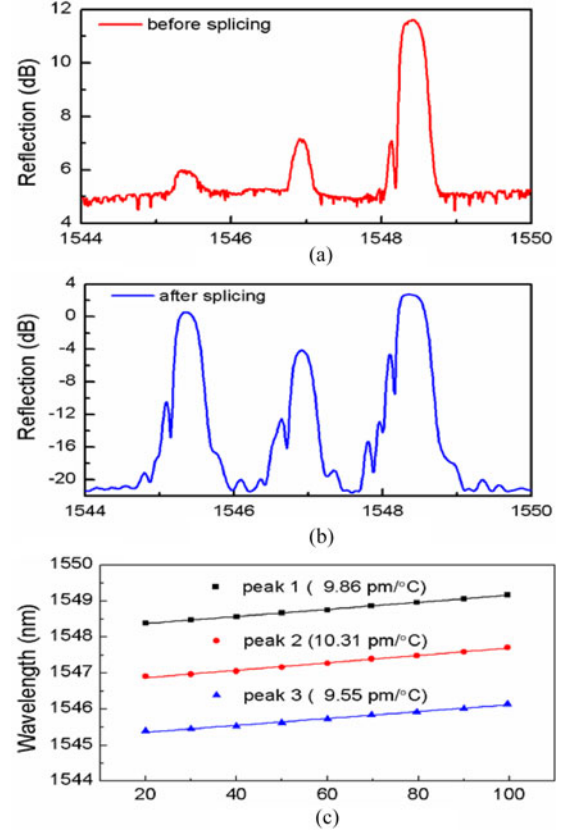


Fig. 5. (a) Reflection spectrum of the TC-FM FBG before splicing. (b) Reflection spectrum of the TC-FM FBG after splicing. (c) Wavelength shifts of the three reflective resonance peaks of the TC-FM FBG as a function of ambient temperature.

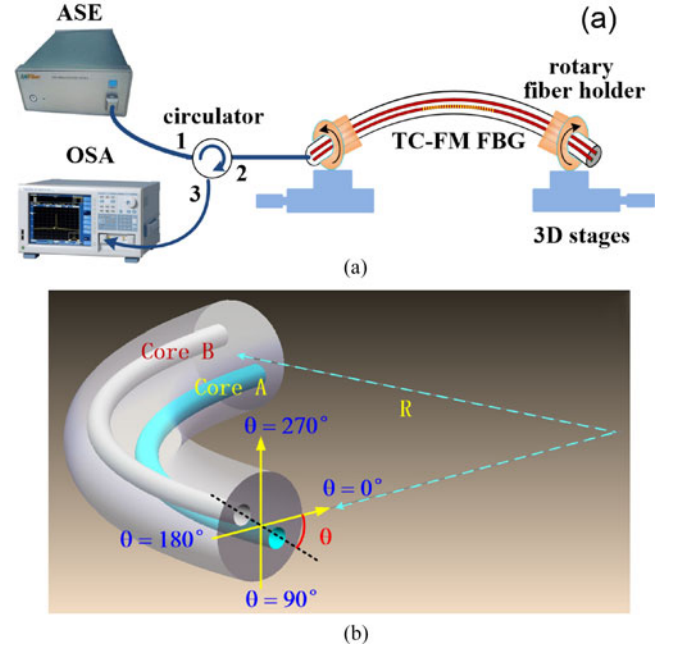


Fig. 6. Schematics of directional bend measurement for TC-FM FBG. (a) Experimental setup. (b) Bend direction with respect to the axis connecting core A and core B in the TC-FMF. Bend direction angle θ is the included angle between the fiber bend plane and the axis connecting core A and core B of the TC-FMF.

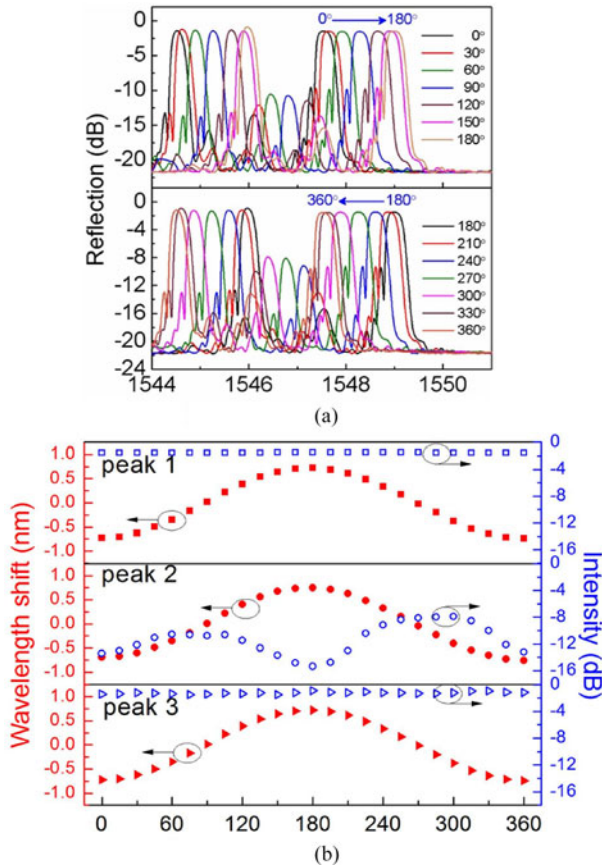


Fig. 7. Bend response of the TC-FM FBG in different bend directions with a constant curvature of 20 m^{-1} . (a) Reflection spectra evolution of the TC-FM FBG with different bend directions (θ : from 0° to 360°). (b) Wavelength shift (left axis) and intensity (right axis) of the three resonance peaks in the reflection spectra of the TC-FM FBG as a function of the bend direction angle θ .

simultaneously. As shown in Fig. 6(b), the bend direction angle θ was defined as the included angle between the bending plane and the axis connecting core A and core B of the TC-FMF. In case θ equals 0° or 360° , the bend direction of TC-FM FBG coincided with the core A and core B axis, and core A was located in the inner side of bent TC-FMF. The reflection spectrum of the TC-FM FBG was recorded when the bend measurement was carried out. Moreover, it should be noted that fiber twisting should be avoided during the bend measurement for TC-FM FBG.

At first, we set a constant bend curvature of 20 m^{-1} for the TC-FM FBG, and changed the bend direction angle θ from 0° to 360° with a step of 15° . It can be seen from Fig. 7 that all of the three resonant wavelengths exhibit ‘red’ shift in case θ changes from 0° to 180° , whereas exhibit ‘blue’ shift in case θ changes from 180° to 360° . The responses of the three resonant wavelengths to the bend direction angle θ could be treated as three similar cosine curves. Moreover, the reflective intensities of peak 1 and 3 corresponding to LP_{01} mode resonance and LP_{11} mode resonance, as shown in Fig. 7(b), could hardly change with different bend direction angles θ . Nevertheless, the reflective intensity of peak 2 corresponding to LP_{01} – LP_{11} mode cross-coupling resonance is sensitive to the bend direction

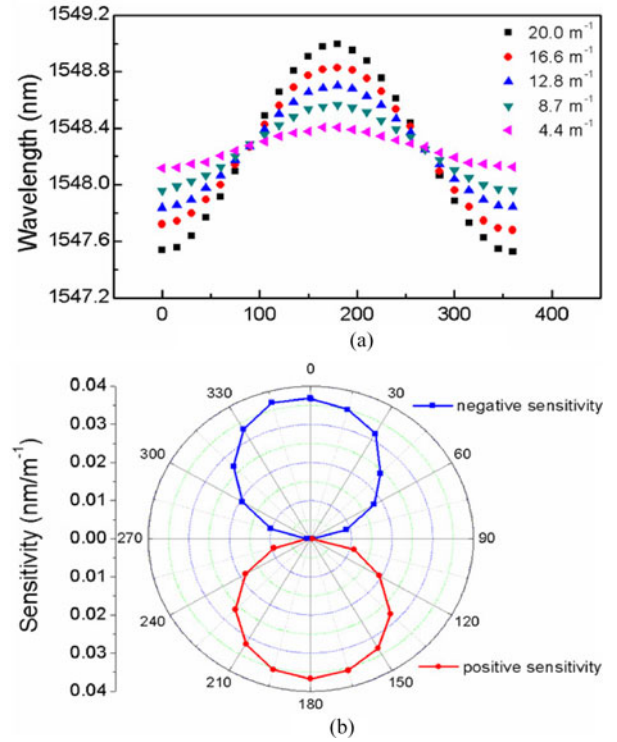


Fig. 8. (a) Resonant wavelength of peak 1 in the reflection spectrum of TC-FM FBG as a function of the bend direction angle θ under different bend curvatures. (b) Bend sensitivities of the TC-FM FBG in different bend directions (θ : from 0° to 360°).

angle θ . This result could further be explored and developed for multi-parameter sensing.

After that, we tested the bend sensitivities of the TC-FM FBG in different bend directions. As shown in Fig. 8(a), the resonant wavelength of peak 1 was recorded with different bend direction angles θ from 0° to 360° with a step of 15° , and repeated measurements were carried out for different bend curvatures from 4.4 to 20.0 m^{-1} . It could be seen from Fig. 8(a) that the bend sensitivities, i.e., the responses of the resonant wavelengths to the bend curvature, are different in different bend directions. We drew the bend sensitivities of the TC-FM FBG with different direction angles θ from 0° to 360° in polar coordinates. A perfect ‘8’ figure could be seen clearly, as shown in Fig. 8(b). It means that the bend sensitivity reaches its maximum in the case of θ equals 0° , 180° , and 360° , whereas the bend sensitivity reaches the minimum and approaches zero in the case of θ equals 90° and 270° . Moreover, the bend sensitivity is negative with a ‘blue’ shift in the resonant wavelength in case of θ between 0° and 90° or θ between 270° and 360° , while the bend sensitivity is positive with a ‘red’ shift in the resonant wavelength in the case of θ between 90° and 270° . Therefore, the TC-FM FBG exhibits the capability of directional bend sensing.

Subsequently, we measured the maximum bend sensitivity of the TC-FMF in the case of θ equals 0° , i.e., TC-FM FBG was bent in the direction along the core A and core B axis, and core A was located in the inner side of the bent TC-FMF. As shown in Fig. 9(a), all of the three resonant wavelengths exhibit ‘blue’ shifts with the increasing bend curvature. Moreover,

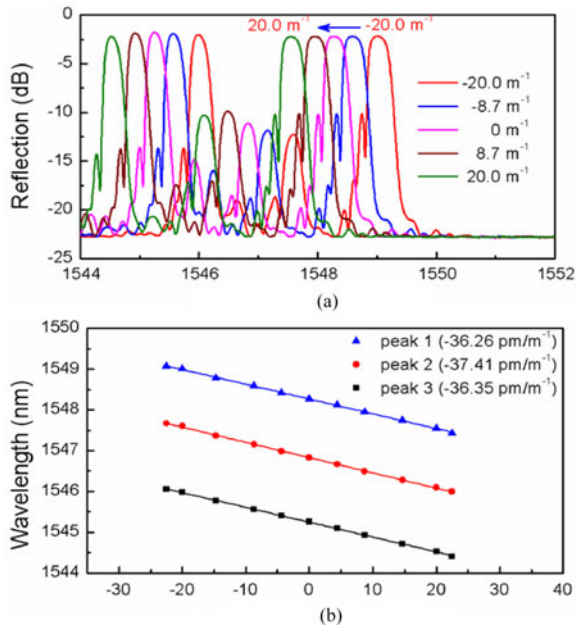


Fig. 9. Bend response of the TC-FM FBG with different bend curvature in the bend direction of θ equals 0° . (a) Reflection spectra evolution of the TC-FM FBG with different bend curvature. (b) Wavelength shift of the three resonance peaks in the reflection spectra of the TC-FM FBG as a function of bend curvature.

we can see from Fig. 9(b) that the three resonant wavelengths, i.e., the peak 1, 2, and 3 corresponding to LP_{01} mode resonance, LP_{01} – LP_{11} mode cross-coupling resonance, and LP_{11} mode resonance, shift linearly with the increasing bend curvature with slightly different bend sensitivities of -36.26 , -37.41 , and -36.35 pm/m^{-1} , respectively.

The bend direction of the TC-FM FBG coincides with the axis connecting core A and core B when θ equals 0° , 180° , and 360° . In the case of θ equals 0° or 360° , the TC-FM FBG is compressed, and the resonance peak reaches the shortest wavelength. In the case of θ evolves from 0° to 180° , the compression in FBG is reduced and the stretching in FBG is increased, and the resonance peak shift towards a longer wavelength, i.e., the ‘red’ shift shown in Fig. 7. In the case of θ equals 180° , the TC-FM FBG is stretched and the resonance peak reaches the longest wavelength. In the case of θ evolves from 180° to 0° , the stretching in FBG is reduced and the compression in FBG is increased, and the resonance peak shift towards a shorter wavelength, i.e., ‘blue’ shift shown in Fig. 7.

Moreover, in the case of θ equals 0° or 360° , the compression in FBG will be increased with a larger bend curvature, and hence exhibits the negative maximum bend sensitivity, as shown in Figs. 8 and 9. On the contrary, in the case of θ equals 180° , the stretching in FBG will be increased with a larger bend curvature, and hence exhibits the positive maximum bend sensitivity, as shown in Fig. 8. In the case of θ equals 90° and 270° , the bend direction of the TC-FM FBG is perpendicular to the axis connecting core A and core B. In this situation, the compression or stretching in FBG will not be affected by the changing bend curvature, and hence exhibits the minimum bend sensitivity of approaching zero, as shown in Fig. 8.

V. CONCLUSION

We have demonstrated femtosecond laser inscription of FBGs in a TC-FMF for directional bend sensing. At first, an FBG was selectively inscribed in one specific core of the TC-FMF using an 800 nm femtosecond laser through a phase mask. And then, the mode excitation in the TC-FMF FBG was studied via offset coupling in a fusion splicer. Three resonance peaks at the wavelengths of 1549.05, 1547.65, and 1546.08 nm were observed in the reflection spectrum, and were responsible for LP_{01} mode resonance, LP_{01} – LP_{11} mode cross-coupling resonance, and LP_{11} mode resonance, respectively. Moreover, the directional bend response of the TC-FM FBG was studied, and the experimental results demonstrated that the TC-FM FBG had the capability of directional bend sensing with a maximum bend sensitivity of -37.41 pm/m^{-1} . Hence, such TC-FM FBGs directional bend sensors could further be developed for promising vector seismic or acoustic detectors and 3D shape sensors.

REFERENCES

- [1] D. J. Richardson, J. M. Fini, and L. E. Nelson, “Space-division multiplexing in optical fibres,” *Nature Photon.*, vol. 7, pp. 354–362, 2013.
- [2] R. G. H. V. Uden *et al.*, “Ultra-high-density spatial division multiplexing with a few-mode multicore fibre,” *Nature Photon.*, vol. 8, pp. 865–870, 2014.
- [3] H. Chen *et al.*, “Integrated cladding-pumped multicore few-mode erbium-doped fibre amplifier for space-division-multiplexed communications,” *Nature Photon.*, vol. 10, pp. 529–533, 2016.
- [4] G. M. H. Flockhart, W. N. MacPherson, J. S. Barton, J. D. C. Jones, L. Zhang, and I. Bennion, “Two-axis bend measurement with Bragg gratings in multicore optical fiber,” *Opt. Lett.*, vol. 28, no. 6, pp. 387–389, 2003.
- [5] E. Lindley *et al.*, “Demonstration of uniform multicore fiber Bragg gratings,” *Opt. Express*, vol. 22, no. 25, pp. 31575–31581, 2014.
- [6] K. Stepien *et al.*, “Fiber Bragg gratings in hole-assisted multicore fiber for space division multiplexing,” *Opt. Lett.*, vol. 39, no. 12, pp. 3571–3574, 2014.
- [7] P. S. Westbrook *et al.*, “Multicore fiber distributed feedback lasers,” *Opt. Lett.*, vol. 37, no. 19, pp. 4014–4016, 2012.
- [8] P. Guo *et al.*, “Inscription of Bragg gratings in few-mode optical fibers,” *Chin. Opt. Lett.*, vol. 11, no. 2, 2013, Art. no. 020606.
- [9] T. Y. Huang, S. N. Fu, C. J. Ke, P. P. Shum, and D. M. Liu, “Characterization of fiber Bragg grating inscribed in few-mode silica-germanate fiber,” *IEEE Photon. Technol. Lett.*, vol. 26, no. 19, pp. 1908–1911, Oct. 2014.
- [10] C. Wu *et al.*, “Strong LP_{01} and LP_{11} mutual coupling conversion in a two-mode fiber Bragg grating,” *IEEE Photon. J.*, vol. 4, no. 4, pp. 1080–1086, Aug. 2012.
- [11] T. Tenderenda *et al.*, “Fiber Bragg grating inscription in few-mode highly birefringent microstructured fiber,” *Opt. Lett.*, vol. 38, no. 13, pp. 2224–2226, 2013.
- [12] J. L. Dong and K. S. Chiang, “Mode-locked fiber laser with transverse-mode selection based on a two-mode FBG,” *IEEE Photon. Technol. Lett.*, vol. 26, no. 17, pp. 1766–1769, Sep. 2014.
- [13] M. J. Gander *et al.*, “Bend measurement using Bragg gratings in multicore fibre,” *Electron. Lett.*, vol. 36, no. 2, pp. 120–121, 2000.
- [14] M. Silva-Lopez *et al.*, “Differential birefringence in Bragg gratings in multicore fiber under transverse stress,” *Opt. Lett.*, vol. 29, no. 19, pp. 2225–2227, 2004.
- [15] M. Silva-López *et al.*, “Transverse load and orientation measurement with multicore fiber bragg gratings,” *Appl. Opt.*, vol. 44, no. 32, pp. 6890–6897, 2005.
- [16] G. M. H. Flockhart, G. A. Cranch, and C. K. Kirkendall, “Differential phase tracking applied to Bragg gratings in multi-core fibre for high accuracy curvature measurement,” *Electron. Lett.*, vol. 42, no. 7, pp. 390–391, 2006.
- [17] A. Fender *et al.*, “Dynamic two-axis curvature measurement using multicore fiber Bragg gratings interrogated by arrayed waveguide gratings,” *Appl. Opt.*, vol. 45, no. 36, pp. 9041–9048, 2006.

- [18] H. L. Zhang *et al.*, "Fiber Bragg gratings in heterogeneous multicore fiber for directional bending sensing," *J. Opt.*, vol. 18, 2016, Art. no. 085705.
- [19] Y. P. Wang and Y. J. Rao, "A novel long period fiber grating sensor measuring curvature and determining bend-direction simultaneously," *IEEE Sens. J.*, vol. 5, no. 5, pp. 839–843, Oct. 2005.
- [20] P. Saffari, T. Allsop, A. Adebayo, D. Webb, R. Haynes, and M. M. Roth, "Long period grating in multicore optical fiber: An ultra-sensitive vector bending sensor for low curvatures," *Opt. Lett.*, vol. 39, no. 12, pp. 3508–3511, 2014.
- [21] T. Guo *et al.*, "Polarization-maintaining fiber-optic-grating vector vibroscope," *Opt. Lett.*, vol. 38, no. 4, pp. 531–533, 2013.
- [22] C. Waltermann, A. Doering, M. Kohring, M. Angelmahr, and W. Schade, "Cladding waveguide gratings in standard single-mode fiber for 3D shape sensing," *Opt. Lett.*, vol. 40, no. 13, pp. 3109–3112, 2015.
- [23] B. Sun *et al.*, "Asymmetrical in-fiber Mach-Zehnder interferometer for curvature measurement," *Opt. Express*, vol. 23, no. 11, pp. 14596–14602, 2015.
- [24] J. Villatoro, V. P. Minkovich, and J. Zubia, "Photonic crystal fiber interferometric vector bending sensor," *Opt. Lett.*, vol. 40, no. 13, pp. 3113–3116, 2015.
- [25] Y. Gong, T. Zhao, Y. J. Rao, and Y. Wu, "All-fiber curvature sensor based on multimode interference," *IEEE Photon. Technol. Lett.*, vol. 23, no. 11, pp. 679–681, Jun. 2011.
- [26] R. Suo *et al.*, "Fiber Bragg gratings inscribed using 800 nm femtosecond laser and a phase mask in single and multi-core mid-IR glass fibers," *Opt. Express*, vol. 17, no. 9, pp. 7540–7548, 2009.
- [27] C. R. Liao, Y. H. Li, D. N. Wang, T. Sun, and K. T. V. Grattan, "Morphology and thermal stability of fiber Bragg gratings for sensor applications written in H₂-free and H₂-loaded fibers by femtosecond laser," *IEEE Sensors J.*, vol. 10, no. 11, pp. 1675–1681, Nov. 2010.
- [28] J. He *et al.*, "Highly birefringent phase-shifted fiber Bragg gratings inscribed with femtosecond laser," *Opt. Lett.*, vol. 40, no. 9, pp. 2008–2011, 2015.
- [29] J. He *et al.*, "Negative-index gratings formed by femtosecond laser overexposure and thermal regeneration," *Sci. Rep.*, vol. 6, 2016, Art. no. 23379.
- [30] C. W. Smelser, S. J. Mihailov, and D. Grobncic, "Formation of type I-IR and type II-IR gratings with an ultrafast IR laser and a phase mask," *Opt. Express*, vol. 13, no. 14, pp. 5377–5386, 2005.
- [31] M. Bernier, S. Gagnon, and R. Vallée, "Role of the 1D optical filamentation process in the writing of first order fiber Bragg gratings with femtosecond pulses at 800 nm [Invited]," *Opt. Mater. Express*, vol. 1, no. 5, pp. 832–844, 2011.
- [32] Y. Lai, K. Zhou, K. Sugden, and I. Bennion, "Point-by-point inscription of first-order fiber Bragg grating for C-band applications," *Opt. Express*, vol. 15, no. 26, pp. 18318–18325, 2007.

Kaiming Yang received the B.S. degree in optical information science and technology from East China JiaoTong University, Nanchang, China, in 2012. He is currently working toward the Ph.D. degree at Shenzhen University, Shenzhen, China. His current research interests include fiber Bragg gratings and femtosecond laser micromachining.

Jun He received the B.Eng. degree in electronic science and technology from Wuhan University, Wuhan, China, in 2006, and the Ph.D. degree in electrical engineering from the Institute of Semiconductors, Chinese Academy of Sciences, Beijing, China, in 2011. From 2011 to 2013, he was with Huawei Technologies, Shenzhen, China, as a Research Engineer. From 2013 to 2015, he was with Shenzhen University, Shenzhen, China, as a Postdoctoral Research Fellow. From 2015 to 2016, he was with the University of New South Wales, Sydney, Australia, as a Visiting Fellow. Since 2017, he has been in Shenzhen University, Shenzhen, China, as an Assistant Professor. His current research interests include optical fiber sensors, fiber Bragg gratings, and fiber lasers. He has authored or coauthored 4 patents and more than 60 journals and conference papers. He is a member of the Optical Society of America.

Changrui Liao received the B.Eng. degree in optical engineering and the M.S. degree in physical electronics from Huazhong University of Science and Technology, Wuhan, China, in 2005 and 2007, respectively, and the Ph.D. degree in electrical engineering from the Hong Kong Polytechnic University, Hong Kong, in 2012. He is currently with Shenzhen University, Shenzhen, China, as an Associate Professor. His current research interests include femtosecond laser micromachining, optical fiber sensors, and optomicrofluidics.

Ying Wang received the B.S. degree in applied physics and the Ph.D. degree in physical electronics from Huazhong University of Science and Technology, Wuhan, China, in 2004 and 2010, respectively. From 2010 to 2015, he worked in the Hong Kong Polytechnic University, Hong Kong, China, as a Research Associate. Since 2015, he has been a Lecturer in Shenzhen University, Shenzhen, China. His research interests include optical fiber sensors and femtosecond laser micromachining.

Shen Liu received the Ph.D. degree from Shenzhen University, Shenzhen, China, in 2017. He is currently a Visiting Fellow at Aston University, Birmingham, U.K.

Kuikui Guo received the B.S. degree from Changchun University of Science and Technology, Changchun, China, in 2013. He is currently working toward the Ph.D. degree at Shenzhen University, Shenzhen, China. From 2013 to 2015, he worked in Accu-Tech Co. Ltd, Beijing, China.

Jiangtao Zhou received the B.S. degree from Anhui Jianzhu University, Hefei, China, in 2012, and the M.S. degree from Shenzhen University, Shenzhen, China, in 2015. He is currently working toward the Ph.D. degree in Ecole Polytechnique Fédérale de Lausanne, Lausanne, Switzerland.

Zhengyong Li received the B.S. degree from Wenhua College of Huazhong University of Science and Technology, Wuhan, China, in 2012, and the M.S. degree from Shenzhen University, Shenzhen, China, in 2015, where he is currently working toward the Ph.D. degree

Zhan Tan received the B.S. degree from Shenzhen University, Shenzhen, China, in 2014, where he is currently working toward the M.S. degree.

Yiping Wang (SM'11) received the B.Eng. degree in precision instrument engineering from Xi'an Institute of Technology, Xi'an, China, in 1995, and the M.S. degree and Ph.D. degree in optical engineering from Chongqing University, China, in 2000 and 2003, respectively. From 2003 to 2005, he was with Shanghai Jiao Tong University, China, as a Postdoctoral Fellow. From 2005 to 2007, he was with the Hong Kong Polytechnic University, as a Postdoctoral Fellow. From 2007 to 2009, he was with the Institute of Photonic Technology, Jena, Germany, as a Humboldt Research Fellow. From 2009 to 2011, he was with the Optoelectronics Research Centre, University of Southampton, Southampton, U.K., as a Marie Curie Fellow. Since 2012, he has been with Shenzhen University, Shenzhen, China, as a Distinguished Professor. His current research interests include optical fiber sensors, fiber gratings, and photonic crystal fibers. He has authored or coauthored 1 book, 21 patent applications, and more than 280 journal and conference papers. He is a Senior Member of the Optical Society of America and the Chinese Optical Society.